*Chemical Geology (Isotope Geoscience Section)*, 65 (1987) 167–181
Elsevier Science Publishers B.V., Amsterdam — Printed in The Netherlands



# ARGON DIFFUSION IN PARTIALLY OUTGASSED ALKALI FELDSPARS: INSIGHTS FROM $^{40}Ar/^{39}Ar$ ANALYSIS

PETER K. ZEITLER

*Research School of Earth Sciences, Australian National University, Canberra, A.C.T. 2601 (Australia)*

(Received August 20, 1986; accepted for publication January 26, 1987)

## Abstract

Zeitler, P.K., 1987. Argon diffusion in partially outgassed alkali feldspars: Insights from $^{40}Ar/^{39}Ar$ analysis. Chem. Geol. (Isot. Geosci. Sect.), 65: 167–181.

Two microclines showing saddle-shaped $^{40}Ar/^{39}Ar$ age spectra, a rapidly cooled orthoclase, and a sanidine from the Fish Canyon Tuff (Colorado, U.S.A.) were subjected to laboratory degassing in an attempt to better understand Ar diffusion systematics in alkali feldspars. The microclines and orthoclase show age spectra that confirm that these samples, and probably most alkali feldspars, comprise diffusion domains of widely varying grain size (greater than a factor of 10). The sanidine shows an age spectrum consistent with the range of grain sizes found in the dated mineral separate. Activation energies derived from the $^{39}Ar$ release are correlated with intensity of outgassing as well as initial structural state. Despite evidence that much of the excess $^{40}Ar$ contained in the microclines is situated near grain boundaries, dry degassing, even at 800 °C, has little effect on this component. However, hydrothermal treatment at 400 °C facilitates significant loss of this excess $^{40}Ar$, providing evidence that it is sited in anion vacancies. The fact that most alkali feldspars are likely to comprise a range of effective grain sizes for diffusion has important implications for the interpretation of age spectra, and will complicate the derivation of diffusion parameters from $^{39}Ar$ released during step-heating.

## 1. Introduction

$^{40}Ar/^{39}Ar$ analysis of alkali feldspar is proving to be a very helpful means of deciphering low-temperature thermal histories (Harrison et al., 1986; Harrison and Bè, 1983). There is now substantial evidence that alkali feldspars reliably record their thermal history, certainly in terms of bulk $^{40}Ar$ loss and age of thermal disturbance. What remains to be explored is how well age spectra obtained from alkali feldspars record nuances in thermal history. To this end, I report results from an ongoing study of Ar diffusion in alkali feldspars. This work, involving application of the $^{40}Ar/^{39}Ar$ step-heating method to alkali feldspars degassed under controlled conditions in the laboratory, had two aims: (1) an assessment of how well theoretical models describe Ar diffusion in real feldspars; and (2) an examination of how episodic heating affects samples originally showing saddle-shaped age spectra.

## 2. Analytical procedures

### 2.1. Samples

Details about three of the four alkali feldspars discussed below (*83-44*, *83-46* and *81-576*) may be found in Zeitler and Fitz Gerald (1986).

0168-9622/87/$03.50 

Two of these samples (*83-44* and *83-46*) show markedly saddle-shaped age spectra as a result of incorporating excess $^{40}Ar$. Transmission electron microscopy (TEM) examination of these samples reveals numerous textures and microstructures. Based on these observations, Zeitler and Fitz Gerald (1986) estimated that both samples *83-44* and *83-46* might have effective grain sizes for diffusion on the order of several micrometers, well under the physical grain sizes of the separates (180–250 and 210–250 $\mu$m). In addition, effective grain sizes vary by a factor of 10 or more, depending on which microstructures are considered to contribute to enhanced rates of diffusion. In both samples, most of the feldspar is maximum microcline, with minor amounts of albite. In sample *83-46*, domains of orthoclase also are present.

Sample *81-576* shows nearly a flat age spectrum, reflecting rapid cooling at $\sim 60\,^{\circ}C\ Ma^{-1}$. Using X-ray powder diffraction, the sample appears to be orthoclase. The fourth feldspar (Fish Canyon, Colorado, U.S.A.) is a sanidine extracted from a welded ash-flow tuff 27.8 Ma in age (Steven et al., 1967). Its $^{40}Ar/^{39}Ar$ age spectrum shows a plateau (J. Sutter, pers. commun., 1985), consistent with concordant 28-Ma apatite and zircon fission-track dates (Naeser et al., 1981) which indicate that the Fish Canyon Tuff has remained well below 100 °C since deposition.

### 2.2. *Heating*

Foland (1974) found no significant difference in Ar diffusion between aliquots of a structurally homogeneous orthoclase degassed in air, under vacuum, or under water pressure. Hence, for convenience and practicality, this study's samples were degassed in several ways. All high-temperature degassing (700 °C for 20 hr. and 800 °C for 23.5 hr.) was done in quartz tubes left open to the atmosphere. The tubes were placed on a ceramic block inside a pre-heated muffle furnace, in which temperature was controlled with a precision of $\pm 5\,^{\circ}C$. Temperature was measured with a thermocouple placed in close proximity to the quartz tubes, and the measured temperatures are probably accurate to within $\pm 30\,^{\circ}C$.

The low-temperature degassing (400 °C) of samples *83-46* and *83-44* was performed in evacuated glass break-seals. Three break-seals were tied together and hung in the center of a tube furnace, with a thermocouple inserted between the three samples. Over the duration of the experiment (1466 hr.), temperature was maintained to $\pm 5\,^{\circ}C$, and the accuracy of the measured temperature is probably $\pm 30\,^{\circ}C$. Following the experiment, the gas evolved into each break-seal during heating was spiked and analyzed as a cross-check on the fraction of Ar lost from the sample. In all three cases, the evolved gas was highly radiogenic, and agreed in quantity with the amount lost from the samples.

One aliquot of sample *83-44* was degassed at 400 °C for 960 hr at 1 kbar water pressure. About 0.6 g of sample was sealed with 40 mg of distilled water in a gold capsule. Temperature in the cold-seal bomb was measured with a thermocouple inserted into the side of the bomb. Over the course of the experiment, temperature varied by $\pm 5\,^{\circ}C$, and was probably measured with an accuracy of $\pm 30\,^{\circ}C$. Some comminution of sample did occur, but no sign of alteration was noted. Before neutron irradiation, fine material was washed away from the sample to minimize the possibility of recoil effects associated with very small grain sizes.

### 2.3. *$^{40}Ar/^{39}Ar$ analysis*

An extraction system new to A.N.U. was used for the analysis of all samples, and a brief summary is provided here. A modified version of the double-vacuum resistance-heated furnace described by Staudacher et al. (1978) and Harrison and Fitz Gerald (1986) is used to heat samples. Temperature is maintained by a temperature controller–thyristor which holds temperature fluctuations to within $\pm 1\,^{\circ}C$.

Preliminary calibration of the crucible suggests that the measured temperature is accurate to within $\pm 10°C$. Gas cleanup is achieved by simultaneous operation of two SAES® getter pumps at 20° and 400°C, with the tantalum crucible tube also contributing somewhat to gettering. Blank levels of $^{40}Ar$ during analysis were $< 3.5 \cdot 10^{-14}$ mol for temperatures of $< 1200°C$, and $\sim 10^{-13}$ mol at higher temperatures; all blanks had a $^{40}Ar/^{36}Ar$ ratio indistinguishable from that of air. Routine throughput is one gas fraction every 40 min., with 12 min. being the effective time spent at temperature for each extraction step.

The purified gas extracted from each sample was analyzed on a VG Isotopes® MM*1200*B mass spectrometer, operated at 2 kV accelerating potential and 105-$\mu$A trap current. Sensitivity of the instrument using the Faraday cup is very stable at $3.5 \cdot 10^{-15}$ mol $mV^{-1}$ ($10^{11}$-$\Omega$ resistor), and constant over the range of sample sizes analyzed in this study. Apparent $^{40}Ar/^{39}Ar$ ages were calculated using the constants recommended by Steiger and Jäger (1977).

Due to delays in commissioning the new Ar-extraction system, considerable time elapsed between irradiation of the samples and their analysis. Consequently, no $^{37}Ar$ was detected, and corrections for Ca-derived nucleogenic interferences could not be made. However, previous analyses of the material used in this study show that these corrections are negligible, and that virtually all $^{39}Ar$ is K-derived and all $^{36}Ar$ is atmospheric in origin.

In obtaining diffusion parameters from $^{39}Ar$ release, spherical geometry was assumed, for reasons given by Zeitler and Fitz Gerald (1986). The equations given by Fechtig and Kalbitzer (1966) were used, and diffusion parameters were obtained using the regression of York (1969). Uncertainties on the cumulative $^{39}Ar$ release were conservatively estimated to be on the order of $\pm 10\%$ or less, yielding uncertainties in $D/a^2$ of $\sim 20$–$40\%$.

## 3. Results

Table I lists all $^{40}Ar/^{39}Ar$ analytical data [analytical data for the untreated aliquots of samples *83-44*, *83-46* and *81-576* may be found in Zeitler and Fitz Gerald (1986)]. Fig. 1 shows the age spectra for degassed aliquots of samples *81-576* and Fish Canyon, along with several theoretical models and the age spectra of the untreated samples. Figs. 2 and 3 show the age spectra of untreated and degassed aliquots of samples *83-44* and *83-46*, along with several intercomparisons of the spectra.

### *3.1. Samples not showing saddle-shaped age spectra*

The degassed aliquots of Fish Canyon sanidine and *81-576* orthoclase show age spectra that are broadly consistent with major and recent Ar loss (Fig. 1). Both samples attain zero apparent age over the first few percent of $^{39}Ar$ release, and then rise to ages which are close to those found in the untreated sample. Both samples lost $\sim 40\%$ of their radiogenic Ar ($^{40}Ar^{\star}$), with the sanidine demonstrating substantially greater Ar retentivity, as it was degassed for 3.5 hr. longer and at temperature 100°C higher than that of *81-576* orthoclase. In detail, the spectra do not agree with model age spectra (Turner, 1968) calculated for 40% episodic Ar loss from homogeneous populations of spheres or slabs (Fig. 1). In particular, the observed age spectra do not show as much upward convexity as predicted by the models, nor do they show lowered ages at high $^{39}Ar$ loss.

### *3.2. Samples showing saddle-shaped age spectra*

A substantial fraction of the Ar contained in samples *83-44* and *83-46* is excess $^{40}Ar$ which is released at very low and at high extraction temperatures, yielding saddle-shaped age spectra. Zeitler and Fitz Gerald (1986) argued that most of this excess $^{40}Ar$ is sited in anion vacancies.

TABLE I

$^{40}Ar/^{39}Ar$ analytical data

| Temperature (°C) | $^{40}Ar$ ($10^{-15}$ mol) | $^{39}Ar$ ($10^{-16}$ mol) | $^{36}Ar$ ($10^{-16}$ mol) | Radiogenic $^{40}Ar$ (%) | Cumulative $^{39}Ar$ (%) | Apparent age $\pm 1\sigma$ (Ma) |
|---|---|---|---|---|---|---|
| *Fish Canyon sanidine, degassed in air at 800° C for 23.5 hr.* (0.4242 g; $J = 0.000742$): | | | | | | |
| 500 | 6,847 | 102 | 233 | −0.5 | 0.1 | −4.8 ±8.9 |
| 575 | 426 | 307 | 15 | −2.0 | 0.3 | −0.4 ±0.4 |
| 625 | 379 | 582 | 13 | −0.9 | 0.8 | −0.1 ±0.3 |
| 675 | 377 | 1,213 | 12 | 5.4 | 1.7 | 0.23 ±0.15 |
| 725 | 468 | 2,249 | 12 | 23.3 | 3.8 | 0.65 ±0.08 |
| 775 | 783 | 3,968 | 12 | 54.3 | 7.2 | 1.43 ±0.03 |
| 825 | 1,746 | 6,448 | 12 | 78.6 | 12.6 | 2.85 ±0.03 |
| 875 | 4,147 | 9,260 | 11 | 91.8 | 20.5 | 5.49 ±0.03 |
| 915 | 7,500 | 10,390 | 11 | 95.5 | 29.3 | 9.20 ±0.05 |
| 950 | 12,040 | 11,590 | 10 | 97.4 | 39.2 | 13.47 ±0.07 |
| 975 | 13,260 | 10,080 | 10 | 97.7 | 47.7 | 17.11 ±0.09 |
| 990 | 12,560 | 8,289 | 9 | 97.7 | 54.8 | 19.68 ±0.10 |
| 1,015 | 13,680 | 8,259 | 9 | 97.8 | 61.8 | 21.54 ±0.11 |
| 1,035 | 13,490 | 7,636 | 10 | 97.7 | 68.3 | 22.95 ±0.12 |
| 1,065 | 15,330 | 8,276 | 11 | 97.8 | 75.3 | 24.09 ±0.13 |
| 1,095 | 19,340 | 9,901 | 11 | 98.1 | 83.7 | 25.45 ±0.13 |
| 1,120 | 18,850 | 9,324 | 10 | 98.3 | 91.7 | 26.38 ±0.14 |
| 1,150 | 16,100 | 7,805 | 11 | 97.8 | 98.3 | 26.79 ±0.14 |
| 1,250 | 4,955 | 1,985 | 26 | 84.3 | 100.0 | 27.94 ±0.17 |
| 1,350 | 3,646 | 42 | 121 | 1.8 | 100.0 | 21 ±20 |
| *81-576 orthoclase, degassed in air at 700° C for 20 hr.* (0.3829 g; $J = 0.000742$): | | | | | | |
| 500 | 1,840 | 318 | 61 | 2.2 | 0.3 | 1.7 ±0.6 |
| 600 | 757 | 2,349 | 26 | −0.8 | 2.2 | −0.03 ±0.09 |
| 680 | 781 | 9,484 | 22 | 15.7 | 9.6 | 0.17 ±0.02 |
| 715 | 1,014 | 12,320 | 15 | 53.9 | 19.3 | 0.59 ±0.01 |
| 745 | 1,624 | 11,437 | 13 | 74.9 | 28.3 | 1.42 ±0.02 |
| 760 | 1,973 | 8,592 | 12 | 81.4 | 35.3 | 2.49 ±0.02 |
| 775 | 2,338 | 7,298 | 12 | 84.1 | 41.1 | 3.60 ±0.03 |
| 790 | 2,564 | 6,333 | 11 | 86.5 | 46.1 | 4.68 ±0.04 |
| 810 | 2,968 | 6,023 | 13 | 87.0 | 50.9 | 5.72 ±0.04 |
| 830 | 3.114 | 5,422 | 13 | 87.7 | 55.2 | 6.73 ±0.04 |
| 870 | 4,116 | 6,184 | 18 | 87.1 | 60.1 | 7.74 ±0.05 |
| 910 | 4,231 | 5,460 | 22 | 84.3 | 64.4 | 8.72 ±0.05 |
| 965 | 4,947 | 5,054 | 41 | 75.5 | 68.4 | 9.86 ±0.06 |
| 1,040 | 10,510 | 9,090 | 110 | 68.9 | 75.7 | 10.62 ±0.06 |
| 1,110 | 13,830 | 11,480 | 154 | 66.9 | 84.8 | 10.75 ±0.06 |
| 1,150 | 15,870 | 11,950 | 209 | 60.9 | 94.2 | 10.78 ±0.06 |
| 1,275 | 9,324 | 6,394 | 139 | 55.9 | 99.3 | 10.87 ±0.07 |
| 1,340 | 1,658 | 840 | 31 | 44.8 | 100.0 | 11.79 ±0.28 |
| *83-44 microcline, degassed at 1-kbar water pressure at 400° C for 960 hr.* (0.2687 g; $J = 0.000614$): | | | | | | |
| 500 | 13,050 | 1,643 | 338 | 23.5 | 2.1 | 20.57 ±0.24 |
| 575 | 5,696 | 3,485 | 30 | 84.5 | 6.7 | 15.22 ±0.09 |
| 625 | 7,822 | 4,060 | 16 | 93.6 | 12.0 | 19.86 ±0.11 |
| 675 | 9,969 | 5,035 | 12 | 96.3 | 18.6 | 20.97 ±0.11 |

TABLE I (*continued*)

| Temperature (°C) | $^{40}Ar$ ($10^{-15}$ mol) | $^{39}Ar$ ($10^{-16}$ mol) | $^{36}Ar$ ($10^{-16}$ mol) | Radiogenic $^{40}Ar$ (%) | Cumulative $^{39}Ar$ (%) | Apparent age $\pm 1\sigma$ (Ma) |
|---|---|---|---|---|---|---|
| *83-44 microcline, degassed at 1-kbar water pressure at 400°C for 960 hr.* (0.2687 g; $J=0.000614$): (cont.) | | | | | | |
| 710 | 9,106 | 4,544 | 12 | 96.1 | 24.4 | 21.20 ± 0.12 |
| 740 | 8,206 | 4,052 | 12 | 95.5 | 29.8 | 21.29 ± 0.11 |
| 790 | 10,560 | 5,089 | 23 | 93.4 | 36.4 | 21.32 ± 0.11 |
| 835 | 10,900 | 5,022 | 35 | 90.4 | 42.9 | 21.58 ± 0.11 |
| 900 | 13,570 | 5,820 | 63 | 86.2 | 50.5 | 22.11 ± 0.12 |
| 965 | 16,980 | 6,376 | 118 | 79.4 | 58.8 | 23.26 ± 0.12 |
| 1,035 | 20,580 | 6,503 | 187 | 73.1 | 67.3 | 25.42 ± 0.14 |
| 1,085 | 21,190 | 5,890 | 207 | 71.0 | 75.0 | 28.06 ± 0.15 |
| 1,135 | 36,650 | 8,993 | 347 | 72.0 | 86.7 | 32.18 ± 0.17 |
| 1,160 | 28,620 | 8,026 | 198 | 79.4 | 97.1 | 31.08 ± 0.17 |
| 1,300 | 6,981 | 2,201 | 42 | 82.1 | 100.0 | 28.60 ± 0.17 |
| *83-44 microcline, degassed in vacuum at 400°C for 1466 hr.* (0.3822 g; $J=0.000608$): | | | | | | |
| 525 | 4,617 | 1,068 | 149 | 4.5 | 1.0 | 2.15 ± 0.18 |
| 600 | 3,491 | 3,239 | 10 | 91.6 | 4.2 | 10.80 ± 0.07 |
| 630 | 5,118 | 3,071 | 5 | 97.0 | 7.3 | 17.64 ± 0.10 |
| 650 | 5,500 | 2,996 | 5 | 97.1 | 10.2 | 19.44 ± 0.11 |
| 670 | 6,023 | 3,165 | 4 | 97.8 | 13.3 | 20.30 ± 0.11 |
| 700 | 8,416 | 4,319 | 6 | 97.8 | 17.7 | 20.77 ± 0.11 |
| 730 | 11,820 | 5,958 | 8 | 97.9 | 23.6 | 21.18 ± 0.11 |
| 755 | 10,690 | 5,343 | 5 | 98.4 | 28.8 | 21.44 ± 0.11 |
| 790 | 13,150 | 6,520 | 6 | 98.6 | 35.2 | 21.68 ± 0.11 |
| 830 | 16,330 | 7,996 | 6 | 98.9 | 43.2 | 21.99 ± 0.11 |
| 870 | 16,920 | 8,164 | 7 | 98.7 | 51.2 | 22.29 ± 0.11 |
| 920 | 17,570 | 8,244 | 7 | 98.7 | 59.4 | 22.93 ± 0.13 |
| 975 | 16,230 | 7,201 | 7 | 98.6 | 66.4 | 24.21 ± 0.12 |
| 1,045 | 18,010 | 7,032 | 8 | 98.7 | 73.5 | 27.49 ± 0.14 |
| 1,100 | 19,870 | 6,463 | 8 | 98.8 | 79.9 | 33.01 ± 0.17 |
| 1,140 | 27,220 | 7,625 | 13 | 98.5 | 87.3 | 38.17 ± 0.20 |
| 1,170 | 31,370 | 9,287 | 17 | 98.3 | 96.5 | 36.06 ± 0.19 |
| 1,250 | 10,300 | 3,517 | 8 | 97.7 | 100.0 | 31.09 ± 0.16 |
| *83-44 microcline, degassed in air at 700°C for 20 hr.* (0.2311 g; $J=0.000741$): | | | | | | |
| 500 | 2,213 | 301 | 76 | −0.9 | 0.4 | −0.9 ± 0.7 |
| 575 | 411 | 1,176 | 14 | 1.5 | 2.0 | 0.07 ± 0.12 |
| 625 | 355 | 2,443 | 11 | 2.8 | 5.2 | 0.06 ± 0.05 |
| 665 | 472 | 3,735 | 10 | 34.8 | 10.0 | 0.59 ± 0.04 |
| 675 | 1,648 | 3,020 | 47 | 16.2 | 14.0 | 1.18 ± 0.05 |
| 715 | 1,947 | 4,731 | 37 | 43.8 | 20.3 | 2.41 ± 0.04 |
| 735 | 2,189 | 4,312 | 27 | 62.8 | 26.0 | 4.26 ± 0.03 |
| 755 | 2,655 | 4,109 | 26 | 70.1 | 31.4 | 6.05 ± 0.05 |
| 770 | 2,935 | 3,610 | 24 | 75.3 | 36.1 | 8.16 ± 0.06 |
| 790 | 3,584 | 3,621 | 27 | 77.6 | 40.9 | 10.23 ± 0.07 |
| 810 | 4,151 | 3,513 | 29 | 79.1 | 45.5 | 12.45 ± 0.09 |
| 840 | 5,070 | 3,896 | 26 | 84.5 | 50.7 | 14.64 ± 0.09 |
| 870 | 5,752 | 3,873 | 29 | 84.9 | 55.7 | 16.78 ± 0.09 |
| 910 | 6,864 | 4,058 | 35 | 84.7 | 61.1 | 19.04 ± 0.11 |
| 960 | 8,089 | 4,324 | 35 | 87.2 | 66.8 | 21.67 ± 0.12 |

TABLE I (*continued*)

| Temperature (°C) | $^{40}Ar$ ($10^{-15}$ mol) | $^{39}Ar$ ($10^{-16}$ mol) | $^{36}Ar$ ($10^{-16}$ mol) | Radiogenic $^{40}Ar$ (%) | Cumulative $^{39}Ar$ (%) | Apparent age $\pm 1\sigma$ (Ma) |
|---|---|---|---|---|---|---|
| *83-44 microcline, degassed in air at 700°C for 20 hr.* (0.2311 g; $J=0.000741$): (cont.) | | | | | | |
| 1,010 | 8,313 | 3,695 | 47 | 83.2 | 71.6 | 24.84 ± 0.13 |
| 1,080 | 11,970 | 4,553 | 54 | 86.6 | 77.6 | 30.18 ± 0.16 |
| 1,170 | 37,880 | 12,556 | 114 | 91.0 | 94.1 | 36.32 ± 0.19 |
| 1,270 | 13,010 | 4,183 | 127 | 71.1 | 99.6 | 29.35 ± 0.16 |
| 1,330 | 3,339 | 131 | 103 | 8.9 | 99.8 | 29.9 ± 2.0 |
| 1,340 | 3,903 | 167 | 118 | 10.5 | 100.0 | 32.5 ± 1.7 |
| *83-44 microcline, degassed in air at 800°C for 23.5 hr.* (0.5601 g; $J=0.000741$): | | | | | | |
| 600 | 3,971 | 4,542 | 135 | −1.1 | 2.5 | −0.13 ± 0.06 |
| 650 | 531 | 6,122 | 17 | −0.2 | 5.8 | 0.00 ± 0.03 |
| 685 | 437 | 8,682 | 14 | 1.1 | 10.5 | 0.01 ± 0.02 |
| 710 | 420 | 9,651 | 11 | 14.7 | 15.8 | 0.09 ± 0.01 |
| 740 | 524 | 11,870 | 12 | 27.3 | 22.3 | 0.16 ± 0.01 |
| 765 | 777 | 13,630 | 12 | 47.9 | 29.7 | 0.36 ± 0.01 |
| 790 | 1,140 | 12,730 | 12 | 67.4 | 36.6 | 0.81 ± 0.01 |
| 815 | 1,773 | 12,380 | 11 | 80.3 | 43.4 | 1.54 ± 0.02 |
| 850 | 3,205 | 13,590 | 12 | 87.6 | 50.8 | 2.76 ± 0.02 |
| 890 | 5,646 | 13,820 | 16 | 91.1 | 58.3 | 4.97 ± 0.03 |
| 950 | 10,350 | 13,760 | 23 | 93.2 | 65.9 | 9.35 ± 0.05 |
| 1,020 | 16,480 | 11,830 | 32 | 94.1 | 72.3 | 17.45 ± 0.09 |
| 1,090 | 25,770 | 11,580 | 52 | 93.9 | 78.6 | 27.7 ± 0.14 |
| 1,130 | 33,960 | 11,630 | 77 | 93.2 | 84.9 | 36.02 ± 0.19 |
| 1,170 | 50,818 | 18,130 | 110 | 93.5 | 94.8 | 34.71 ± 0.18 |
| 1,300 | 22,410 | 9,539 | 49 | 93.4 | 99.9 | 29.12 ± 0.15 |
| 1,330 | 733 | 171 | 11 | 54.5 | 100.0 | 31.0 ± 0.9 |
| *83-46 microcline, degassed in vacuum at 400°C for 1466 hr.* (0.2807 g; $J=0.000636$): | | | | | | |
| 400 | 670 | 18 | 23 | −0.8 | 0.1 | −3.7 ± 6.6 |
| 475 | 414 | 92 | 13 | 3.8 | 0.3 | 1.9 ± 1.7 |
| 525 | 121 | 139 | 3 | 26.6 | 0.8 | 2.7 ± 0.8 |
| 575 | 442 | 279 | 4 | 73.7 | 1.6 | 13.3 ± 0.5 |
| 625 | 1,370 | 484 | 7 | 85.6 | 3.1 | 27.6 ± 0.2 |
| 690 | 5,249 | 1,357 | 14 | 92.1 | 7.2 | 40.4 ± 0.2 |
| 740 | 4,623 | 1,967 | 8 | 94.7 | 13.1 | 25.35 ± 0.15 |
| 775 | 4,615 | 2,077 | 7 | 95.5 | 19.4 | 24.16 ± 0.14 |
| 810 | 50,750 | 2,343 | 1,841 | < 0.0 | 26.4 | leak |
| 860 | 7,335 | 3,172 | 11 | 95.6 | 36.0 | 25.17 ± 0.14 |
| 900 | 6,560 | 2,807 | 10 | 95.5 | 44.5 | 25.41 ± 0.14 |
| 940 | 6,422 | 2,610 | 11 | 95.0 | 52.4 | 26.61 ± 0.15 |
| 980 | 7,093 | 2,541 | 14 | 94.0 | 60.0 | 29.83 ± 0.16 |
| 1,020 | 8,946 | 2,637 | 18 | 94.0 | 68.0 | 36.21 ± 0.19 |
| 1,060 | 25,620 | 4,261 | 53 | 93.9 | 80.9 | 63.6 ± 0.3 |
| 1,100 | 21,810 | 2,824 | 41 | 94.4 | 89.4 | 81.7 ± 0.4 |
| 1,150 | 23,490 | 2,989 | 45 | 94.3 | 98.4 | 93.0 ± 0.4 |
| 1,300 | 5,283 | 538 | 14 | 92.1 | 100.0 | 100.7 ± 0.6 |

Amounts listed corrected for decay and discrimination. $^{40}Ar$ corrected using $(^{40}Ar/^{39}Ar)_K = 0.027$. Line blanks not removed. Samples shielded in 0.2 mm of Cd during irradiation at HIFAR® reactor, Lucas Heights, Sydney, N.S.W. Flux monitor was GA*1550* biotite (K-Ar age = 97.8 Ma). Errors in age include error in $J$ of 0.5%. Typical relative precisions for peak-height extrapolations: $> 1.0 \cdot 10^{-12}$ mol, ± 0.1% or better; $2.0 \cdot 10^{-15}$ mol, ± 3%.

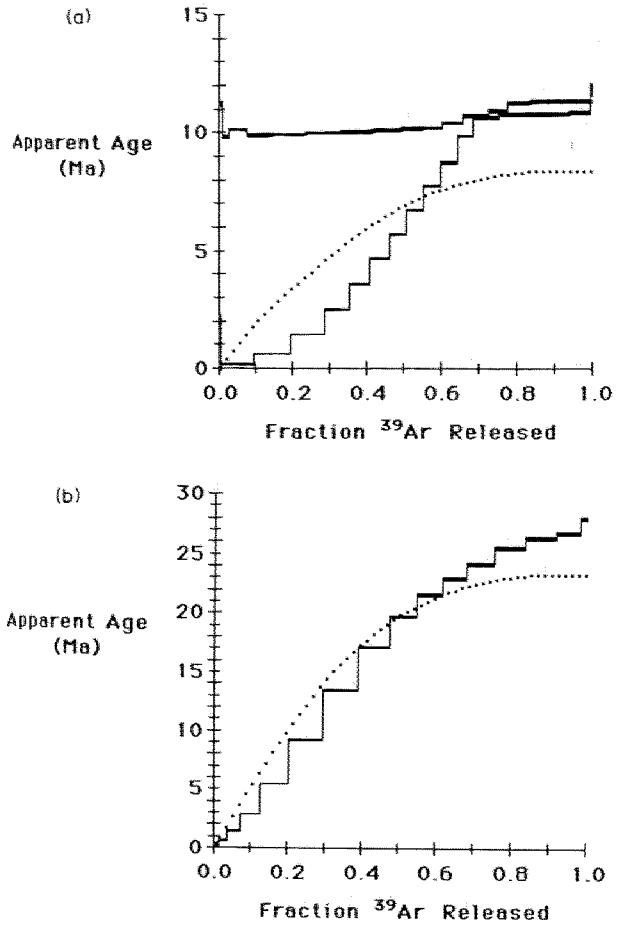


Fig. 1. $^{40}Ar/^{39}Ar$ age spectra of samples not containing excess $^{40}Ar$:
a. Age spectra for untreated and heated aliquots of *81-576* orthoclase. *Dotted line* shows synthetic age spectrum for population of uniform spheres outgassed by 44%.
b. Age spectra for untreated and heated aliquots of Fish Canyon sanidine. *Dotted line* shows synthetic age spectrum for population of uniform spheres outgassed by 40%.

Following the earlier work of Harrison and McDougall (1981) and Claesson and Roddick (1983), they suggested that such siting could explain the observed release of most excess $^{40}Ar$ at high temperatures, despite its apparent location near grain boundaries.

Those aliquots of samples *83-44* and *83-46* degassed under dry conditions show age spectra that reflect episodic Ar loss, complications associated with the excess $^{40}Ar$ aside. Ignoring for a moment the higher-$^{39}Ar$-release portions of their age spectra, samples degassed at successively higher temperatures show progres-

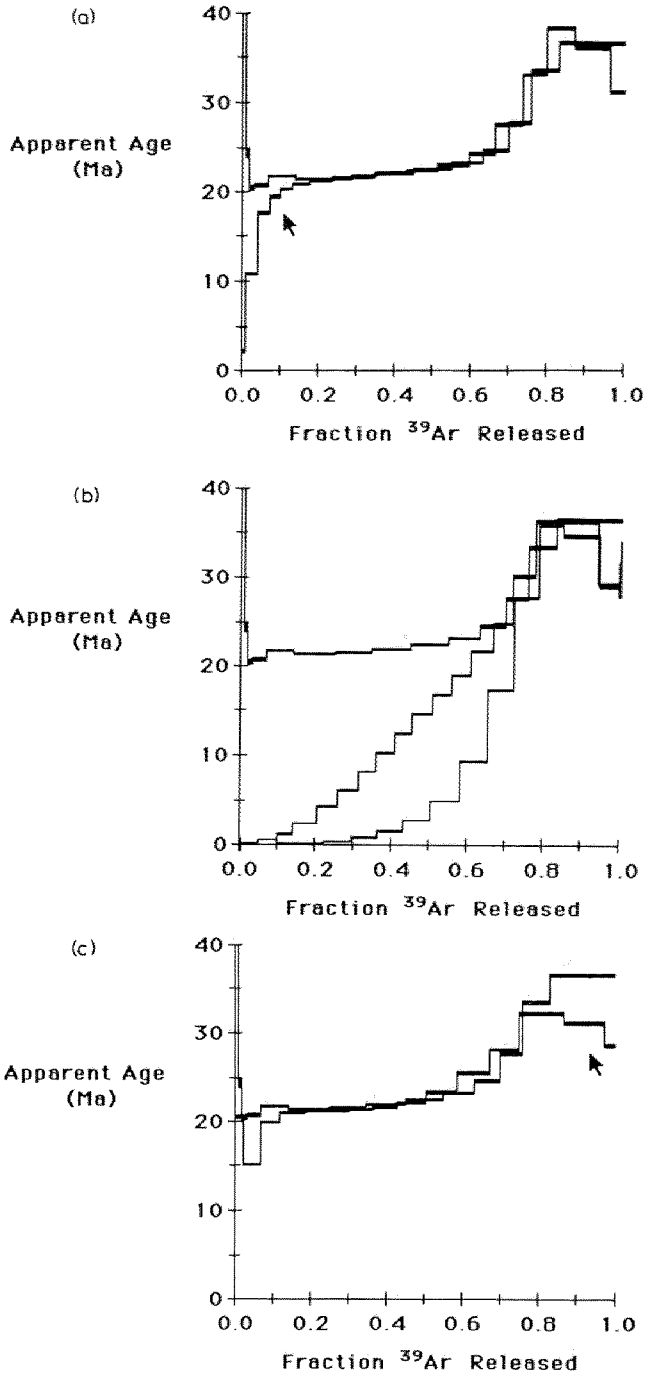


Fig. 2. $^{40}Ar/^{39}Ar$ age spectra for *83-44* microcline:
a. Age spectra for untreated aliquot, and for split outgassed under vacuum at 400°C, showing 4% loss of $^{40}Ar$ (*arrow*).
b. Age spectra for untreated aliquot, and for splits outgassed in air at 700° and 800°C.
c. Age spectra for untreated aliquot, and split degassed at 1-kbar water pressure, 400°C. The presence of water during low-temperature outgassing appears to have facilitated loss of a $^{40}Ar$ component normally released at high temperatures under dry conditions (*arrow*).

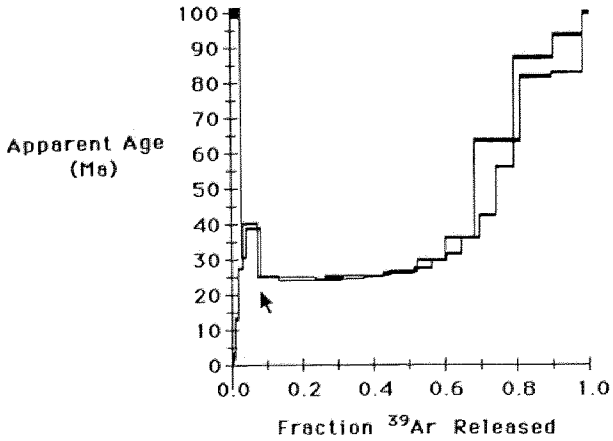


Fig. 3. $^{40}Ar/^{39}Ar$ age spectra for untreated and heated aliquots of *83-46* microcline. Note the partial degassing of the excess-$^{40}Ar$ gradient expressed at low $^{39}Ar$ release in the untreated split (*arrow*).

sively greater amounts of $^{40}Ar$ loss (Fig. 2). At low $^{39}Ar$ release, their age spectra either achieve or extrapolate to an apparent age of zero, and in the case of the aliquots of *83-44* degassed at higher temperatures, the zero-age portions of the age spectra extend over 5% or more $^{39}Ar$ release. Further, for both samples *83-44* and *83-46*, the high ages present at low $^{39}Ar$ release in the undisturbed samples are missing from the age spectra of the degassed specimens, proving that the high ages are due to excess $^{40}Ar$, and not loss of $^{39}Ar$ by recoil. In fact, comparison of the heated and untreated aliquots of *83-46* (Fig. 3) reveals that much of the $^{40}Ar$ loss in this sample represents degassing of an Ar-gain profile of the sort proposed by Harrison and McDougall (1980).

In contrast to the Ar loss manifested at low extraction temperatures, dry degassing did not diminish the amount of excess $^{40}Ar$ released at high temperatures (Table II). Even the 800 °C run, which yielded a 55% loss of total $^{40}Ar$, and which reset ages to nearly zero over the first 30% of $^{39}Ar$ release, showed only a 6% loss of $^{40}Ar$ above 75% $^{39}Ar$ release.

The aliquot of sample *83-44* degassed under water pressure at 400 °C stands apart from the others, as it expresses markedly lowered ages at high levels of $^{39}Ar$ release. It appears that the presence of water during prolonged low-temperature heating facilitated partial loss of that component of excess $^{40}Ar$ found to be resistant to dry degassing, even at 800 °C. At low extraction temperatures, the sample shows an age spectrum consistent with minor loss of $^{40}Ar^{\star}$, with the elevated ages found at the lowest extraction temperatures possibly indicating minor recoil loss of $^{39}Ar$ from the separate.

### *3.3. Diffusion parameters*

Table III gives diffusion parameters derived from the $^{39}Ar$ released during the step-heating experiments. As is commonly observed in alkali feldspars, apparent diffusivities obtained at high temperatures fall increasingly below those that would be predicted by an ideal Arrhenius relationship (Fig. 4). In several of the samples, this seems to occur continuously, even at lower temperatures. Thus, the parameters reported in Table III are merely estimates, based as they are on only the few points measured at temperatures below 725 °C.

It is worth noting, however, that the activation energies obtained for sample *83-44* are correlated with intensity of outgassing. This may reflect an increase in Si,Al disorder in response to heating to temperatures of 700 °C and above [Cherry and Trembath (1979) found that Si,Al disordering began after as little as 12 hr. of dry heating at 1025 °C]. Note that the activation energies for higher-temperature runs (51.3 and 50.8 kcal.) are close to the value derived for Fish Canyon sanidine (50.4 kcal.). Further, the split of sample *83-44* degassed hydrothermally at 400 °C yields the lowest activation energy of all (34.3 kcal.), perhaps because the presence of water facilitated complete ordering of all domains to maximum microcline. If so, the data presented in Table III provide evidence that the rate of Ar diffusion in alkali feldspars is dependent on structural state.

## 4. Discussion

### *4.1. Age spectrum shape*

Grain-size variation can drastically modify the shape of age spectra. Turner (1968) and

TABLE II

$^{40}$Ar losses

| Sample | Heating conditions[*1] | Bulk loss[*2] (%) | Deficit (%) at $^{39}$Ar release of[*3] | |
|---|---|---|---|---|
| | | | >40% | >75% |
| Fish Canyon | 23.5 hr., 800°C | 40 | | |
| *81-576* | 20 hr.; 700°C | 44 | | |
| *83-44* | 23.5 hr.; 800°C | 55 | 33 | 6 |
| *83-44* | 20 hr.; 700°C | 35 | 9 | 0 |
| *83-44* | 1,466 hr.; 400°C | 4 | 0 | 0 |
| *83-44* | 960 hr.; 400°C; wet | 7 | 5 | 11 |
| *83-46* | 1,466 hr.; 400°C | 18 | 0 | 7 |

[*1]All but one sample heated dry, in air or under vacuum (see text). Hydrothermal run at 1 kbar water pressure.
[*2]Losses ± two percentage units.
[*3]For samples containing excess $^{40}$Ar and showing saddle-shaped age spectra, deficit in $^{40}$Ar with respect to untreated sample, over region indicated.

TABLE III

Diffusion parameters

| Sample[*1] | | | Activation energy[*2] (kcal. ± 1σ) | ln($D_0/a^2$) ± 1σ[*2] |
|---|---|---|---|---|
| *83-44* | (400°C, wet) | (3) | 34.3 ± 0.2 | 5.7 ± 2.4 |
| *83-44* | (400°C, dry) | (6) | 43.6 ± 1.7 | 9.6 ± 1.9 |
| *83-44* | (700°C) | (6) | 51.3 ± 1.6 | 13.5 ± 1.8 |
| *83.44* | (800°C) | (4) | 50.8 ± 3.3 | 12.8 ± 3.5 |
| *83-46* | (400°C, dry) | (6) | 41.7 ± 1.1 | 7.2 ± 1.2 |
| *81-576* | (700°C) | (4) | 63.9 ± 4.8 | 20.1 ± 2.4 |
| Fish Canyon | (800°C) | (8) | 50.4 ± 0.9 | 9.6 ± 0.9 |

[*1]Value in brackets gives number of points in regression.
[*2]Diffusion parameters based on regression of all data obtained at 725°C and below, assuming a homogeneous population of spheres, and an extraction duration of 12 min. per step. Results for Fish Canyon calculated from data obtained at 875°C and below.

more recently Gillespie et al. (1982) have shown that under conditions of episodic heating, a range in grain sizes yields very different age spectra than does a homogeneous population, particularly at high levels of outgassing (Fig. 5). Many workers have suggested that the effective grain size for diffusion in alkali feldspars is controlled by microstructures, and will thus be smaller than the physical grain size of the mineral separate. Foland (1974) pointed out that as a result of microstructural control, effective grain sizes on the order of 1–10 $\mu$m are probably common in perthitic alkali feldspars, and TEM examination indeed reveals domains of this size to be common in alkali feldspars (e.g., Parsons and Brown, 1983; Zeitler and Fitz Gerald, 1986). However, as many fine-scale exsolution lamellae are often considered to be coherent of semicoherent, it is not clear to what extent they actually serve to define effective diffusion dimension.

Model age spectra which take grain-size vari-

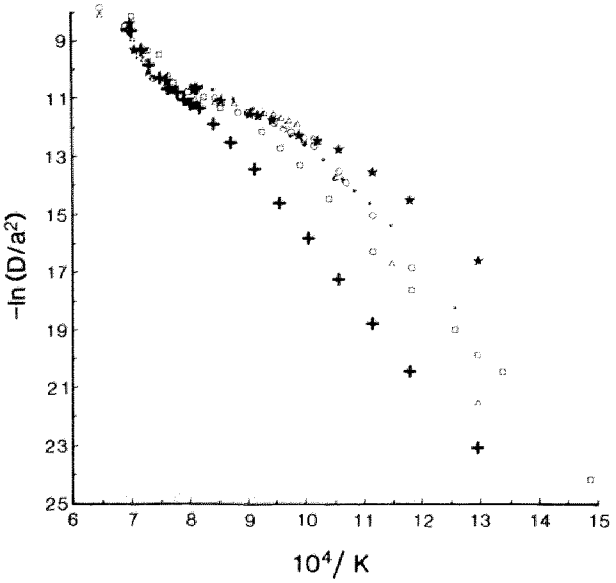


Fig. 4. Arrhenius plot derived from the $^{39}$Ar released by the samples during step-heating. *Symbols*: *crosses* = Fish Canyon; *triangles* = *81-576* (700°C); *squares* = *83-46* (400°C); *circles* = *83-44* (700°C); *open stars* = *83-44* (800°C); *asterisks* = *83-44* (400°C); *solid stars* = *83-44* (400°C, 1 kbar wet).

ation into account (Fig. 6) are in far better agreement with the age spectra of samples *81-576* and Fish Canyon than those models based on uniform populations of spheres or slabs (Fig. 1). For Fish Canyon, the mismatch in ages at high $^{39}$Ar release probably signifies that a component of large grains was omitted from the model. For both samples, minor shifts in the relative weighting of each size fraction could be used to force better fits. Because Fish Canyon sanidine was assumed to be a homogeneous feldspar, the grain-size distribution of the dated mineral separate was used for modelling. For sample *81-576*, two grain sizes differing by a factor of 10 were used, each size being weighted equally by volume.

One can make a simple limiting calculation to determine the magnitude of the grain-size

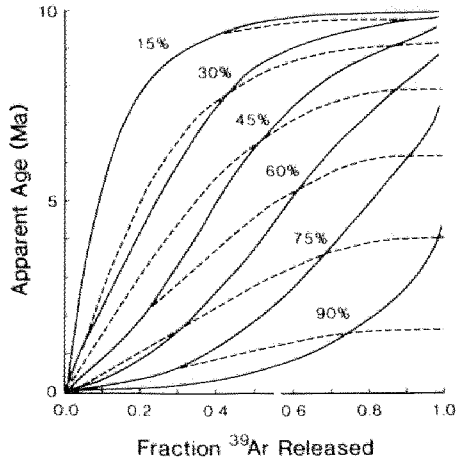


Fig. 5. Synthetic age spectra for recent episodic loss from populations of spheres, obtained using method of Turner (1968). Values given are percent $^{40}$Ar loss. *Dotted curves* = single grain size; *solid curves* = 10 grain sizes equally weighted by volume, largest size 10× smallest size.

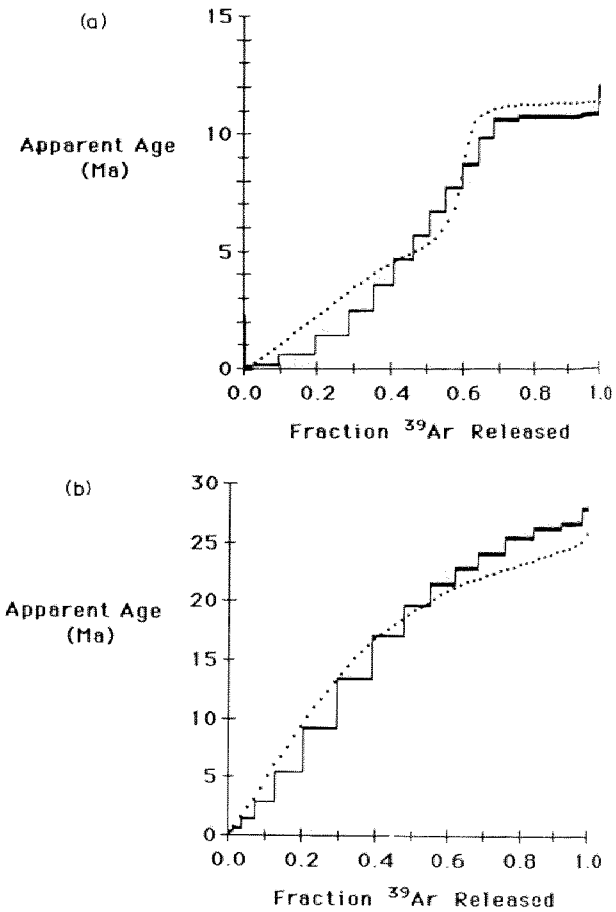


Fig. 6. a. Age spectrum for degassed split of *81-576* orthoclase, and synthetic age spectrum (*dotted line*) for 44% $^{40}$Ar loss, assuming two grain sizes different by a factor of 10, and equally weighted by volume.
b. Age spectrum for degassed split of Fish Canyon sanidine, and synthetic age spectrum (*dotted line*) for 40% $^{40}$Ar loss, assuming physical grain size distribution found in the dated separate.

variation found within sample *81-576*. From examination of the sample's age spectrum (Table I; Fig. 1), it appears that the smallest domains were outgassed by at least 95% and the largest domains by no more than 5%. For spheres, these levels of outgassing correspond to $Dt/a^2$-values of 0.253 and $2.18 \cdot 10^{-4}$, respectively. If the difference in these values is entirely attributable to grain radius, the two grain sizes would need to differ by only a factor of ~35. Such a variation in grain size is quite plausible, given that the physical grain size of *81-576* alkali feldspar ranged between 124 and 178 $\mu$m, and that numerous potential diffusion domains on the order of 1 $\mu$m or smaller in size are commonly observed in alkali feldspars (e.g., Parsons and Brown, 1983; Zeitler and Fitz Gerald, 1986).

Although no attempt was made to model the samples containing excess $^{40}$Ar, it is apparent from Fig. 2 that the more heavily outgassed aliquots show concave-upward age spectra attributable to a range in grain sizes. Further, the basalt-entrained granite xenoliths analyzed by Gillespie et al. (1983, 1984) show similar concave-upward spectra, again suggesting that natural samples consist of a wide range of effective diffusion domains.

The $^{40}$Ar/$^{39}$Ar age spectra of partially outgassed alkali feldspars are strong evidence that a considerable range in diffusion dimensions is present within most samples. This observation indicates that microstructures do divide grains into domains having effective dimensions on the order of 10 $\mu$m or less, and that Ar transport along microstructural boundaries is rapid compared to volume diffusion. The complicated diffusion systematics in a metamorphic hornblende reported by Harrison and Fitz Gerald (1986) supports this conclusion, as effective diffusion dimensions of as small as 0.3 $\mu$m are required to explain their observations.

### 4.2. Implications of grain-size variation

Based on the evidence discussed above as well as the many studies that have been made of microstructures in alkali feldspar, it seems inevitable that with the exception of some high-temperature feldspars, each grain in a typical alkali feldspar separate will comprise several diffusion domains of varying sizes. This leads to several observations on the interpretation of $^{40}$Ar/$^{39}$Ar systematics in alkali feldspars.

First, given the high probability that the grain-size distribution within any feldspar specimen will be unique, rigorous extraction of useful thermochronometric information from the fine structure of $^{40}$Ar/$^{39}$Ar age spectra will be unlikely, for the influence of grain-size distribution will far outweigh that of subtle variations in thermal history [compare the theoretical age spectra shown in Fig. 5 with the age spectra predicted by Harrison (1983) for multiple episodic events]. As more data are accumulated for alkali feldspars, it might become possible to generalize about grain-size distributions, but at present the only option available is exhaustive TEM characterization of effective grain sizes for a representative suite of grains.

Some benefits do accrue from the fact that most alkali feldspars will comprise a range in effective grain sizes for diffusion. In cases of episodic heating, it should be possible to estimate the time of heating with somewhat greater confidence than might be expected from simple models of Ar loss. Simple models assuming homogeneous slabs or spheres show asymptotic approaches to the age axis on an age-spectrum diagram, but except in cases of very small $^{40}$Ar loss, heterogeneous populations yield spectra that approach the age axis more directly (e.g., Fig. 2a). Also, for any given degree of Ar loss, assemblages of varied grain size tend to preserve a better record of their original age (Fig. 5).

A second observation is that grain-size distribution will modify the shape of the age spectra shown by slowly cooled samples. Slow cooling of homogeneous populations will yield spectra that are broadly similar in shape to those observed in response to episodic heating, and

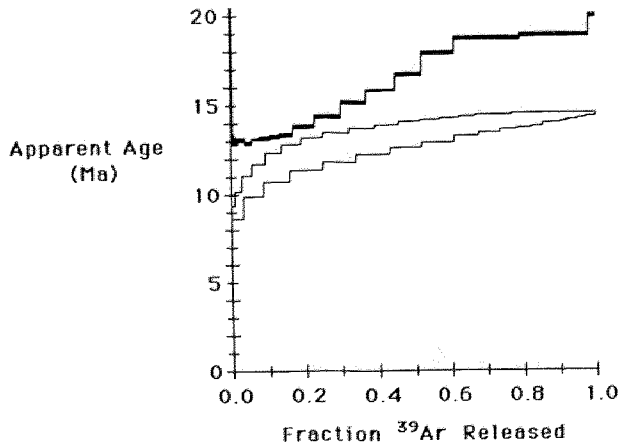


Fig. 7. Synthetic and measured age spectra for slow cooling. *Top curve* (*bold*) age spectrum of alkali feldspar from the northwestern Himalaya, cooled at ~15 °C $Ma^{-1}$ (Zeitler, 1985). *Center curve* = synthetic age spectrum for a homogeneous population of spheres undergoing slow cooling at 15 °C $Ma^{-1}$. *Bottom curve* = synthetic age spectrum for population of spheres undergoing slow cooling at 15 °C $Ma^{-1}$ (parameters as for Fig. 5).

which rise with upward convexity to a plateau (Harrison and McDougall, 1982; Dodson, 1982; Zeitler, 1985). In contrast, alkali feldspars containing a range of grain sizes show age spectra marked by a rather linear increase in age, which never achieves a plateau (Fig. 7).

Finally, the presence of a range of grain sizes within most alkali feldspars will complicate the extraction of diffusion information from them (Fechtig et al., 1963). One can think of Arrhenius plots derived from such samples as representing the weighted average of a series of parallel lines, one for each grain size. At low temperatures, no grain-size reservoirs are depleted, and small grains dominate the release of gas, explaining the good linear arrays often observed at temperatures below 800 °C. As each grain-size reservoir is exhausted during step-heating, the next larger one will dominate the gas release. Overall, a curved pattern will result, and such curved Arrhenius relationships are nearly ubiquitous for all but high-temperature feldspars. This deviation from linearity has often been ascribed to structural changes during the diffusion experiment, such as disordering or homogenization of exsolution lamellae. However, although structural changes all work towards lower-than-expected diffusivities at high temperatures, most of the non-linearity commonly displayed by alkali feldspars can be completely accounted for by a relatively narrow range in grain size (Fig. 8a).

The activation energy derived from the low-temperature linear portion of such an Arrhenius plot will be close to correct, but the frequency factor will be applicable only to relatively small Ar losses. If geologic outgassing is sufficient to deplete the smallest grains of Ar, then the heating conditions responsible for the observed loss will not be successfully predicted using the diffusion parameters derived from only the lowest-temperature extraction steps. The extent to which this effect is significant will depend on the range in grain size, and the volume fraction of each size. Samples with extremely wide ranges in grain size, or a relatively small volume fraction of small diffusion domains, will yield very poorly aligned Arrhenius relationships applicable to a narrow range of Ar losses. Samples marked by a limited range of grain sizes, for example, a sanidine, will yield very good alignments applicable to relatively broad range of Ar losses. In general, the diffusion parameters derived from the lower-temperature steps can be applied to geologic heating events which have integrated $Dt/a^2$-values below that at which the laboratory-derived Arrhenius relationship deviates from linearity.

An interesting and perhaps counter-intuitive consequence of grain-size variation is that in order to maximize the diffusion information obtained from a sample, that is, to extend the linear portion of an Arrhenius relationship over the greatest possible temperature range, it is important to keep extraction steps as brief as is consistent with accurate estimation of heating-step duration (Fig. 8b). The goal is to reach higher temperatures with as low a cumulative $Dt/a^2$ as possible. Many past studies have used heating durations of as long as 1 hr. per step, and such durations would deplete small grain

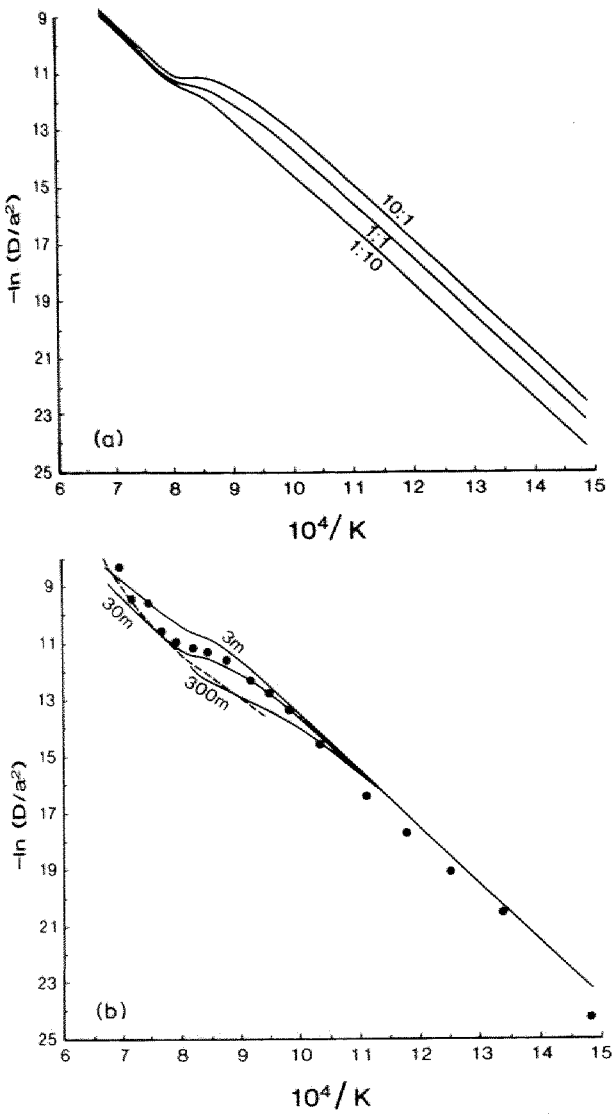


Fig. 8. Arrhenius plots derived from simulated step-heating of samples containing a range in effective grain size for diffusion:
a. Influence of grain-size distribution. *Center curve* = parameters as for Fig. 5. *Top curve* = weighted so that smallest grains 10× more abundant by volume than largest grains. *Bottom curve* = largest grains 10× more abundant by volume than smallest grains.
b. Influence of heating duration. *Top curve* = heating duration 3 min. per step. *Center curve* = heating duration 30 min. per step. *Bottom curve* = heating duration 300 min. per step. *Heavy dashed line* connects location on each curve of $Dt/a^2 = 0.05$ (equivalent to 61% loss of Ar). *Points* show diffusion of $^{39}$Ar from *83-46* (400°C).

sizes of Ar-containing particles at significantly lower temperatures than a heating schedule such as the one used in this study (12 min. at prescribed temperature).

### *4.3. Siting of excess argon*

Saddle-shaped age spectra in feldspars (e.g., Figs 2 and 3) have been attributed to the siting of excess $^{40}$Ar in anion vacancies (Harrison and McDougall, 1981; Claesson and Roddick, 1983). Zeitler and Fitz Gerald (1986), noting that oxygen self-diffusion is extremely slow under dry conditions, suggested that saddle-shaped spectra are laboratory artifacts. They hypothesized that diffusion of excess $^{40}$Ar into anion vacancies is facilitated under natural conditions by the presence of water, but that its release in the Ar-extraction system is greatly inhibited by the dry environment which must prevail under ultra-high vacuum.

At 400°C, hydrothermal degassing of sample *83-44* was able to induce significant loss of that excess-$^{40}$Ar component normally extracted only at high temperatures, and the observed water-dependence of diffusivity is strong evidence that this component is located in anion vacancies. In feldspars, diffusion of alkalis is basically insensitive to water pressure, whereas oxygen diffusion is extremely dependent on the presence of water, and moderately dependent on actual water pressure (Yund, 1983). Thus, detrital alkali feldspars originally showing saddle-shaped age spectra will not compromise the interpretation, for example, of the age spectra of samples undergoing reheating under natural conditions in a sedimentary basin, as prolonged heating in the presence of water would probably lead to outgassing of any anion-sited excess $^{40}$Ar. Further hydrothermal degassing experiments on other minerals known to show saddle-shaped age spectra, such as hornblende, would be of great interest.

## 5. Conclusions

Laboratory degassing experiments on several specimens of alkali feldspar lead to the following conclusions:

(1) The age spectra presented in this study confirm that significant internal grain-size variation is likely to be common in alkali feld-

spar. Interpretations of age spectra obtained from most alkali feldspars will need to take this phenomenon into account. Because grain-size variation plays an important role in altering the shape of $^{40}Ar/^{39}Ar$ age spectra, it will be difficult to extract fine-scale information about temperature history from alkali feldspar age spectra.

(2) Under conditions of episodic heating, grain-size variation does have the beneficial effect of allowing age spectra to more tenaciously preserve information about original age and to yield a more confident estimate of time of heating.

(3) Even moderate grain-size variation can adequately explain the non-linear Arrhenius behavior often displayed by alkali feldspars. Strictly, diffusion parameters obtained from the linear lower-temperature portions of such Arrhenius trends cannot be used to extract time-temperature information from samples which have suffered high levels of Ar loss.

(4) A correlation between observed activation energy and intensity of experimental outgassing suggests that in alkali feldspars, activation energy for Ar diffusion is a function of structural state.

(5) Low-temperature hydrothermal outgassing of an excess $^{40}Ar$ component that under anhydrous conditions is only released at high temperatures provides evidence that this component is sited in anion vacancies. Such a component would probably be removed during heating in most geologic environments, and would not survive to cause problems in age-spectrum interpretation.

## Acknowledgements

Thanks to Ian McDougall and Mark Harrison for comments on this manuscript, and to Terry Davies and Bill Hibberson for technial assistance. I am grateful to Ian McDougall for the excellent facilities he has made available to me. Irradiations were made possible by a grant from the Australian Institute of Nuclear Science and Engineering (AINSE).

## References

Cherry, M.E. and Trembath, L.T., 1979. The disordering of alkali feldspars, I. Dry heating of a microcline perthite. Can. Mineral., 17: 527-535.

Claesson, S. and Roddick, J.C., 1983. $^{40}Ar/^{39}Ar$ data on the age and metamorphism of the Ottfjället dolerites, Särv Nappe, Swedish Caledonides. Lithos, 16: 61-73.

Crank, J., 1975. The Mathematics of Diffusion. Clarendon, Oxford, 2nd ed., 414 pp.

Dodson, M.H., 1982. Closure profiles in cooling mineral grains. 5th Int. Conf. on Geochronology, Cosmochronology, and Isotope Geology, Nikko National Park, June 27-July 2, 1982 (abstract).

Fechtig, H. and Kalbitzer, S., 1966. The diffusion of argon in potassium-bearing solids. In: O.A. Schaeffer and J. Zähringer (Editors), Potassium Argon Dating. Springer, Berlin, pp. 68-106.

Fechtig, H., Gentner, W. and Lämmerzahl, P., 1963. Argonbestimmungen an Kaliummineralien, XII. Edelgasdiffusionsmessungen an Stein- und Eisenmeteoriten. Geochim. Cosmochim. Acta, 27: 1149-1169.

Fitz Gerald, J.D. and McLaren, A.C., 1982. The microstructure of microcline from granitic rocks and pegmatites. Contrib. Mineral. Petrol., 80: 219-229.

Foland, K.A., 1974. $^{40}Ar$ diffusion in homogeneous orthoclase and an interpretation of Ar diffusion in K-feldspars. Geochim. Cosmochim. Acta, 38: 151-166.

Gillespie, A.R., Huneke, J.C. and Wasserburg, G.J., 1982. An assessment of $^{40}Ar/^{39}Ar$ dating of incompletely degassed xenoliths. J. Geophys. Res., 87: 9247-9257.

Gillespie, A.R., Huneke, J.C. and Wasserburg, G.J., 1983. Eruption age of a Pleistocene basalt from $^{40}Ar/^{39}Ar$ analysis of partially degassed xenoliths. J. Geophys. Res., 88: 4997-5008.

Gillespie, A.R., Huneke, J.C. and Wasserburg, G.J., 1984. Eruption age of a ~100,00-year-old basalt from $^{40}Ar/^{39}Ar$ analysis of partially degassed xenoliths. J. Geophys. Res., 89: 1033-1048.

Harrison, T.M., 1983. Some observations of the interpretation of $^{40}Ar/^{39}Ar$ spectra. Isot. Geosci., 1: 319-338.

Harrison, T.M. and Bè, K., 1983. $^{40}Ar/^{39}Ar$ age spectrum analysis of detrital microclines from the southern San Joaquin Basin, California: an approach to determining the thermal evolution of sedimentary basins. Earth Planet Sci. Lett., 64: 244-256.

Harrison, T.M. and Fitz Gerald, J.D., 1986. Exsolution in hornblende and its consequences for $^{40}Ar/^{39}Ar$ age spectra and closure temperature. Geochim. Cosmochim. Acta, 50: 247-253.

Harrison, T.M. and McDougall, I., 1980. Investigations of an intrusive contact, northwest Nelson, New Zealand, II. Diffusion of radiogenic and excess $^{40}Ar$ in horn-

blende revealed by $^{40}Ar/^{39}Ar$ age spectrum analysis. Geochim. Cosmochim. Acta, 44: 2005–2020.

Harrison, T.M. and McDougall, I., 1981. Excess $^{40}Ar$ in metamorphic rocks from Broken Hill, New South Wales: implications for $^{40}Ar/^{39}Ar$ age spectra and the thermal history of the region. Earth Planet. Sci. Lett., 55: 123–149.

Harrison, T.M. and McDougall, I., 1982. The thermal significance of potassium feldspar K–Ar ages inferred from $^{40}Ar/^{39}Ar$ age spectrum results. Geochim. Cosmochim. Acta, 46: 1811–1820.

Harrison, T.M., Morgan, P. and Blackwell, D.D., 1986. Constraints on the age of heating at the Fenton Hill Site, Valles Caldera, New Mexico. J. Geophys. Res., 91: 1899–1908.

Naeser, C.W., Zimmerman, R.A. and Cebula, G.T., 1981. Fission-track dating of apatite and zircon: An interlaboratory comparison. Nuclear Tracks, 5: 65–72.

Parsons, I. and Brown, W.L., 1983. A TEM and microprobe study of a two-perthite alkali gabbro: Implications for the ternary feldspar system. Contrib. Mineral. Petrol., 82: 1–12.

Staudacher, T., Jessberger, E.K., Dorflinger, D. and Kiko, J., 1978. A refined ultrahigh vacuum furnace for rare-gas analysis. J. Phys. E. Sci. Instrum., 11: 781–789.

Steiger, R.H. and Jäger, E., 1977. Subcommission on Geochronology: Convention on the use of decay constants in geo- and cosmochronology. Earth Planet. Sci. Lett., 36: 359–362.

Steven, T.A., Mehnert, H.H. and Obradovich, J.D., 1967. Age of volcanic activity in the San Juan Mountains, Colorado. U.S. Geol. Surv., Prof. Pap., 575-D: 47–55.

Turner, G., 1968. The distribution of potassium and argon in chondrites. In: L.H. Ahrens (Editor), Origin and Distribution of the Elements. Pergamon, Oxford, pp. 387–398.

York, D., 1969. Least squares fitting of a straight line with correlated errors. Earth Planet. Sci. Lett., 5: 320–324.

Yund, R.A., 1983. Diffusion in feldspars. In: P.H. Ribbe (Editor), Feldspar Mineralogy. Mineralogical Society of America, Washington, D.C., 2nd ed., pp. 203–222.

Zeitler, P.K., 1985. Numerical modelling of argon diffusion and $^{40}Ar/^{39}Ar$ age spectra. Res. School Earth Sci., Aust. Natl. Univ., Canberra, A.C.T. (unpublished manuscript).

Zeitler, P.K. and Fitz Gerald, J.D., 1986. Saddle-shaped $^{40}Ar/^{39}Ar$ age spectra from young, microstructurally complex potassium feldspars. Geochim. Cosmochim. Acta, 50: 1185–1199.